

Study of the Two Null Nearby Divertor magnetic configuration at EAST

C. Meineri¹, R. Lombroni²

¹ ENEA, *Fusion and Technologies for Nuclear Safety Department, C.R. Frascati, via E. Fermi 45, 00044, Frascati (Rome), Italy*

² *Department of Economics, Engineering, Society and Business Organization (DEIm), University of Tuscia, Largo dell'Università snc, Viterbo, 01100, Italy*

Introduction

Alternative configurations such as Snowflake [1] (SF) and the X-Divertor (XD) [2], have the aim of controlling and optimising the magnetic flux expansion and the connection length. The magnetic configuration XD or ‘Two Null nearby divertor’ (TNND), is created by inducing a secondary X-point outside the divertor region, downstream of the main X-point, with the beneficial effect of increase the field line lengths and the flux expansion from the core X-point to the wall. This positive gradient in flux expansion toward the target is called poloidal flaring, for the divergent character of the field lines. These reduce the peak power flux and the temperature at the strike points. This work try to understand what are the possible effects acting on the reduction of power deposited on the target during the discharge #48971 at tokamak The EAST [3], the only closed null experimental TNND L-mode ,realised in 2014, with NBI external heating. Due to lack of other experimental closed nulls TNND, it has been done a comparison with other two magnetic configurations, the TNND_1 and TNND_2 (Fig.1), where it has been moved the second null at different distance to compare different poloidal flaring. These two configurations are realised with MAXFEA 2D MHD, a non-linear equilibrium solver [4]. In table 1 are summarised the main properties compared in this work. The data of shot #47038, experimental lower single null L-mode with LH external heating, are used as reference, having similar parameter to the TNND_2 but different strike point position as Fig.1.

table 1: main parameters for the different TNND studied

| | X-point separation between two nulls | Grazing angle | Connection Length (m) | Poloidal flux expansion |
|--------|--------------------------------------|---------------|-----------------------|-------------------------|
| 48971 | ~78 cm | ~0.35 | ~200 | ~10 |
| TNND_1 | ~82 cm | ~0.55 | 176 | 8.4 |
| TNND_2 | > 1m | ~1.15 | 145 | 4.0 |
| 47038 | LSN | ~1.22 | 144.38 | 2.01 |

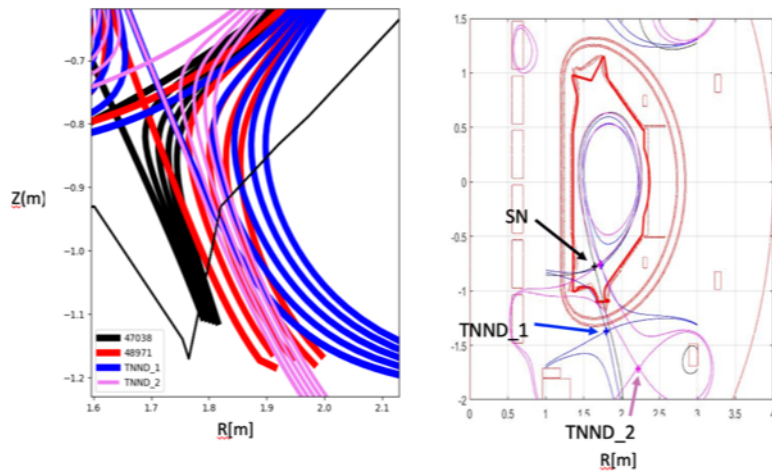


Fig.1: Plasma boundary of analysed equilibria (on the left), the experimental discharges #48971 (red line) and #47038 (black line), the TNND_1 (blue line) and the TNND_2 (violet line). On the right the position of the second null of The TNND_1 and TNND2 respect to #47038 SN case.

Modeling of TNNDs with EMC3-EIRENE

EMC3-EIRENE [5] is an edge code which can study particle and energy transport in the Scrape-Off-Layer. It works with the Monte-Carlo method to solve the Braginskii equation. The three equilibrium has been modelled in EMC3-EIRENE using constant radial density-driven particle and heat diffusion coefficient, $D = 0.5$ and $X = 0.5 \text{ m}^2/\text{s}$, to compare the results of #48971 with previous study done with TECXY and EDGE2D [2]. Total input power across the core boundary was set to 400 kW for both configurations, equally shared between ions and electrons. In EMC3 the volumetric recombination is still neglected, however, so-called ‘molecular assisted recombination’ (MAR) is accounted for by the molecular charge exchange process followed by recombination of molecular ions, see table 1 in reference [6] for the full list of reactions used in EIRENE. These simulations has been based on a simplified particle balance in which the recycling is scaled automatically in order to match the request upstream density, $0.6 \times 10^{19} \text{ m}^{-3}$.

Analysis

The fig.2 compares the power flux density (MW/m^2) deposited on the Outer-Target for the three configuration simulated, with the experimental data obtained from IR-camera for discharge #48971(red dot) and #47038 (black dot). Unfortunately the Langmuir-Probe data are not available. There is a good agreement between #48971 simulation and experimental signal (respectively red continuous lines and dot). The TNND_2 (violet continued curve) is in agreement with #47038 IR-data, showing a non significative influence of its second null on the Power exhaust. The TNND_1 (blue continued curve) shows an intermediate behaviour. The reduction of the heat flux deposit on the Outer-Target its not only caused by a geometrical effect (different inclination of the field line on target) but also a reduction of parallel heat flux Q_{par} (Fig.2 on the right) dependent from the distance of the two nulls. A possible explanation could be the beneficial effect of the increasing of gradient of flux expansion along field line: the index DI_{sol} [7] calculates the flux expansion increase between the main X-point and the strike point

$$DI_{\text{sol}} \equiv \frac{d_b/B_b}{d_a/B_a} = \frac{B_a}{B_b} \frac{d_b}{d_a}$$

where d is the distance between the main X-point and the field lines (\mathbf{a} is the nearest point and \mathbf{b} is the strike point) and B is the poloidal magnetic field. If $DI > 1$, the flux surface are more flared than a SN and if $DI < 1$ it is more contracted than a SN. It table 2 are summarised the different value for DI_{sol} .

table 2: index DI_{sol} for the different magnetic configurations

| | DI_{sol} |
|--------|------------|
| 48971 | 3 |
| TNND_1 | 2.25 |
| TNND_2 | 1.6 |
| 47038 | ~ 1 |

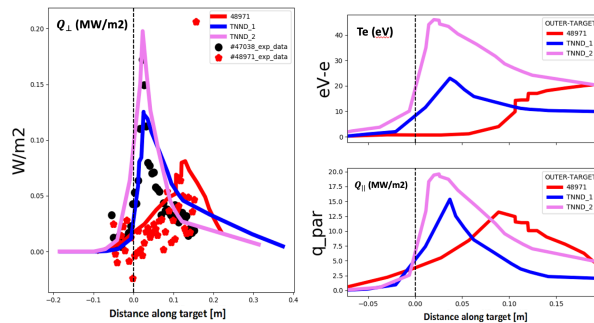


Fig.2: EMC3 target profiles for TNND_1, TNND_2 and #48971 cases at $0.6e19 \text{ m}^{-3}$ at upstream. The #48971 exhibits the onset of the detachment with lower temperatures (Te in eV), lower parallel heat flux (Q_{\parallel} in MW/m²) and a reduction of density power deposited on the target (on the left) compared with experimental data (dotted profiles)

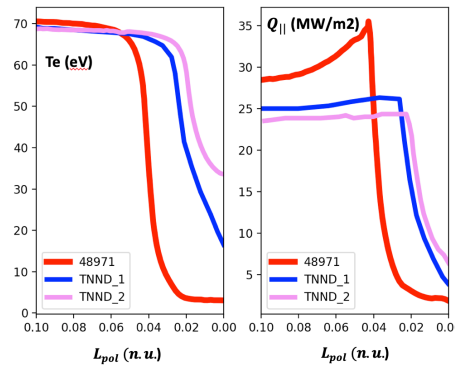


Fig.3: EMC3 poloidal profiles for TNND_1, TNND_2 and #48971 cases at $0.6e19 \text{ m}^{-3}$ at upstream. L_{pol} is the distance along the poloidal field line to the target normalised at 1 to compare the data, with zero as the target position.

Fig. 3 is a collection of poloidal profiles of the three cases at the density of $0.6e19 \text{ m}^{-3}$. The positive gradient of flux expansion (flaring) of the #48971 respect to TNND_1 case, result in a much steeper gradients in temperature (fig.3 on the left) and Q_{\parallel} (fig.3 on the right), as expected. The #48971 withstand the migration of volumetric power losses to the core, insulating the core from target. This difference may be caused also by a deeper detachment, need to be studied. Fig. 4 shows the Electron Temperature and Parallel heat flux, respectively on the left and on the right, at power input of 2MW in function of the electron density on the separatrix at MidPlane; As expected the more flaring geometry reduces the two physical quantities an lower density than other two cases.

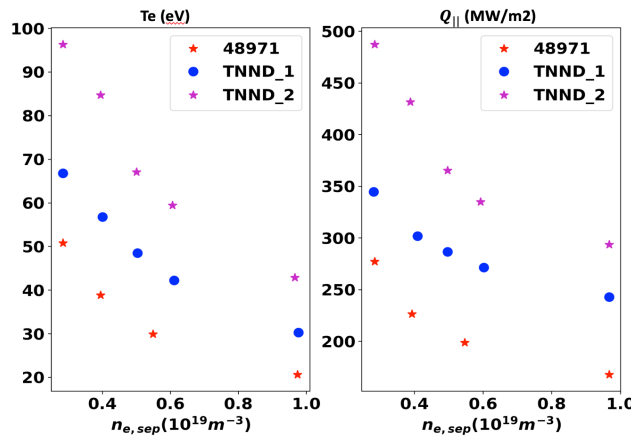


Fig.4: EMC3 peak Electron temperature and parallel heat flux on the target in function of the density at separatrix in Midplane.

Conclusion

EMC3 cannot describe the fully detachment condition, but the power balance shows that an increase of the total power lost for Charge-exchange change from 12% in case with a contract poloidal magnetic field (TNND_2) to a 45% lost in #48971 case, at the onset of detachment, showing that more is the flaring of magnetic geometry more increase the Momentum lost of ion Background with Neutral collision, Important condition for the roll-over of Detachment.

TNNs on EAST tokamak suggested that target flux expansion and flaring could be the responsible of the detachment density threshold. EMC3 models have given interpretation of these observations, by showing how TNNs and the other two cases differently dissipate energy and momentum in the divertor volume due to their geometries. It is clear, that poloidal flux expansion and flaring must work together creating an efficient neutral trapping to see a lower density threshold for detachment, increasing the neutral-ion collisions.

Acknowledgement

This work has been carried out within the framework of the EUROfusion Consortium and has received funding from the Euratom research and training programme 2014-2018 and 2019-2020 under grant agreement No 633053.. The views and opinions expressed herein do not necessarily reflect those of the European Commission

The authors gratefully acknowledge the support and the courtesy of the EAST tokamak diagnostic group.

All the simulation was performed on the CRESCO/ENEAGRID High Performance Computing Infrastructure

References

- [1] Ryutov D.D., et al, Phys Plasmas 15 (2008) 092501
- [2] M. Kotschenreuther, P. Valanju, J. Wiley, T. Rognlein, S. Mahajan, M. Pekker, Proceedings of the 20th International Conference on Fusion Energy, Vilamoura, Portugal (International Atomic Energy Agency, Vienna, (2004).
- [3] G. Calabro, et al., Nucl. Fusion 55 (2015) 083005
- [4] Barabaschi, P., 1993 "The MAXFEA code", Proceedings Plasma Control Technical Meeting, Naka, Japan, April 1993.
- [6] Y. Feng, et al., Contrib. Plasma Phys. 54(4-6), 426-431 (2014)
- [7] M. Kotschenreuther, et al., Phys. Plasmas 20, 102507, 102507